Preparations, Structures, and Magnetic Properties of a Series of Novel Copper(II)−Lanthanide(III) Coordination Polymers via Hydrothermal Reaction

Yucang Liang, Maochun Hong,* Weiping Su, Rong Cao,* and Wenjian Zhang

State Key Laboratory of Structural Chemistry, Fujian Institute of Research on the Structure of Matter, Chinese Academy of Sciences, Fuzhou, Fujian 350002, P. R. China

Received January 24, 2001

The hydrothermal reaction of Ln_2O_3 (Ln = Er, Gd, and Sm), pyridine-2,5-dicarboxylic acid (H_2pydc), and Cu(II) reagents (CuO, $Cu(OAc)_2{\cdot}2H_2O$, or $CuCl_2{\cdot}2H_2O$) with a mole ratio of 1:2:4 resulted in the formation of six polymeric Cu(II)−Ln(III) complexes, $[\{Ln_2Cu_3(pydc)_6(H_2O)_{12}\}{\cdot}4H_2O]_n$ (Ln = Er (**1**); Ln = Gd (**2**)), $[\{Ln_4Cu_2(pydc)_8(H_2O)_{12}\}{\cdot}4H_2O]_n$ (Ln = Sm (**3**); Ln = Gd (**4**); Ln = Er (**5**)), and $[\{Gd_2Cu_2(pydc)_4(H_2O)_8\}{\cdot}Cu(pydc)_2{\cdot}12H_2O]_n$ (**6**). **1** and **2** are isomorphous and crystallize in triclinic space group $P\bar{1}$. Compounds **3**−**5** are isomorphous and crystallize in monoclinic space group $P2_1/c$. Compound **6** crystallizes in triclinic space group $P\bar{1}$. Complexes **1** and **2** have one-dimensional zigzag chain structures and compounds **3**−**5** display three-dimensional wavelike polymeric structures, while **6** has an infinite sandwich-type structure. The different structures of the complexes are induced by the different forms of Cu(II) reagents; the reactions of $Cu(OAc)_2{\cdot}2H_2O$ yield high Cu/Ln ratio products **1**, **2**, and **6**, while the reactions of CuO or $CuCl_2{\cdot}2H_2O$/2,2′-bipyridine results in low Cu/Ln ratio compounds **3**−**5**. Temperature-dependent magnetic susceptibilities for **2**, **4**, and **5** were studied, and the thermal stabilities of complexes **2** and **4** were examined.

Introduction

The coordination chemistry of heterometallic lanthanide−transition metal compounds has been extensively studied since 1985, not only due to their applications in the investigation of the nature of magnetic exchange interaction between 3d and 4f metal ions of magnetic materials containing rare earth metals[1−6] but also because of the fascinating coordination properties of Ln(III).[7] Since the high coordination number of Ln(III) may render structural flexibility and increase the thermodynamic stablity,[8] a great number of structure types of lanthanide−transition metal complexes have been reported. However, although some infinite lanthanide(III)−transition metal compounds obtained by the conventional self-assembly reaction in solution were reported,[1−6,9−24] studies on polymeric compounds,

* Corresponding authors. Fax for M.C.H.: (+86)-591-314946. E-mail for M.C.H.: hmc@ms.fjirsm.ac.cn.

(1) Doble, D. M. J.; Benison, C. H.; Blake, A. J.; Fenske, D.; Jackson, M. S.; Kay, R. D.; Li, W.-S.; SchrÖder, M. *Angew. Chem.* **1999**, *111*, 2042; *Angew. Chem., Int. Ed. Engl.* **1999**, *38*, 1915.
(2) Lisowski, J.; Starynowicz, P. *Inorg. Chem.* **1999**, *38*, 1351.
(3) (a) Blake, A. J.; Gould, R. O.; Grant, C. M.; Milne, P. E. Y.; Parsons, S.; Winpenny, R. E. P. *J. Chem. Soc., Dalton Trans.* **1997**, 485. (b) Brechin, E. K.; Harris, S. G.; Parsons, S.; Winpenny, R. E. P. *J. Chem. Soc., Dalton Trans.* **1997**, 1665.
(4) Costes, J.-P.; Dahan, F.; Dupuis, A.; Laurent, J.-P. *Inorg. Chem.* **1997**, *36*, 3429.
(5) (a) Chen, X.-M.; Aubin, S. M. J.; Wu, Y.-L.; Yang, Y.-S.; Mak, T. C. W.; Hendrickson, D. N. *J. Am. Chem. Soc.* **1995**, *117*, 9600. (b) Chen, X.-M.; Wu, Y.-L.; Yang, Y.-Y.; Aubin, S. M. J.; Hendrickson, D. N. *Inorg. Chem.* **1998**, *37*, 6186. (c) Liu, Q.-D.; Gao, S.; Li, J.-R.; Zhou, Q.-Z.; Yu, K.-B.; Ma, B.-Q.; Zhang, S.-W.; Zhang X.-X.; Jin, T.-Z. *Inorg. Chem.* **2000**, 39, 2488.
(6) (a) Bencini, A.; Benelli, C.; Caneschi, A.; Carlin, R. L.; Dei, A.; Gatteschi, D. *J. Am. Chem. Soc.* **1985**, *107*, 8128. (b) Bencini, A.; Benelli, C.; Caneschi, A.; Dei, A.; Gatteschi, D. *Inorg. Chem.* **1986**, *25*, 572. (c) Benelli, C.; Caneschi, A.; Gatteschi,; D.; Guillou, O.; Pardi, L. *Inorg. Chem.* **1990**, *29*, 1750.
(7) (a) Choppin, G. R. In *Lanthanide Probes in Life, Chemical and Earth Sciences;* Bünzli, J.-C. G., Choppin, G. R., Eds; Elsevier Publishing Co.: Amsterdam, 1989; Chapter 1. (b) Drew, M. G. B. *Coord. Chem. Rev.* **1977**, *24*, 179. (c) Bünzli, J.-C. G. In *Rare Earths*; Saez-Puche, R., Caro, P., Eds.; Editorial Complutense: Madrid, 1998; pp 223−259. (d) Piguet C.; Bünzli, J.-C. G.; *Chem. Soc. Rev.* **1999,** *28*, 347.
(8) (a) Martell, A. E.; Hancock, R. D.; Motekaitis. R. J. *Coord. Chem. Rev.* **1994**, *133*, 39. (b) Lehn, J.-M. *Angew. Chem., Int. Ed. Engl.* **1988**, *27*, 89. (c) Cram, D. J. *Angew. Chem., Int. Ed. Engl.* **1988**, *27*, 1009.
(9) (a) Andruh, M.; Ramade, I.; Codjovi, E.; Guillou, O.; Kahn, O.; Trombe, J. C. *J. Am. Chem. Soc.* **1993**, *115*, 1822. (b) Liu, Q.-D.; Li, J.-R.; Gao, S.; Ma, B.-Q.; Zhou, Q.-Z.; Yu, K.-B.; Liu, H. *Chem. Commun.* **2000**, 1685.
(10) Ramade, I.; Kahn, O.; Jeannin, Y.; Robert, F. *Inorg. Chem.* **1997**, *36*, 930.
(11) (a) Sanz, J. L.; Ruiz., R.; Gleizes, A.; Lloret, F.; Faus, J.; Julve, M.; Borrás-Almenar, J. J.; Journaux, Y. *Inorg. Chem.* **1996**, *35*, 7384. (b) Costes, J.-P.; Dahan, F.; Dupuis, A.; Laurent, J.-P. *Inorg. Chem.* **1996**, *35*, 2400.
(12) (a) Yukawa, Y.; Igarashi, S.; Yamano, A.; Sato, S. *Chem. Commun.* **1997**, 711. (b) Benelli, C.; Blake, A. J.; Milne, P. E. Y.; Rawson, J. M.; Winpenny, R. E. P. *Chem. Eur. J.* **1995**, *1*, 614. (c) Blake, A. J.; Milne, P. E. Y.; Thornton, P.; Winpenny, R. E. P. *Angew. Chem., Int. Ed. Engl.* **1991**, *30*, 1139.
(13) (a) Cui, Y.; Chen, J.-T.; Long, D.-L.; Zheng, F.-K.; Cheng, W.-D.; Huang, J.-S. *J. Chem. Soc., Dalton Trans.* **1998**, 2955. (b) Cui, Y.; Zheng, F.-K.; Huang, J.-S. *Chem. Lett.* **1999**, 281.
(14) Sakagami, N.; Okamoto, K. *Chem. Lett.* **1998**, 201.
(15) Igarashi, S.; Hoshino, Y.; Masuda, Y.; Yukawa, Y. *Inorg. Chem.* **2000**, *39*, 2509.
(16) Loosli, A.; Wermuth, M.; and Güdel, H.-U. *Inorg. Chem.* **2000**, *39*, 2289.
(17) Navarro J. A. R.; Salas, J. M. *Chem. Commun.* **2000**, 235.
(18) Chen, Q.-Y.; Luo, Q.-H.; Wang, Z.-L.; Chen, J.-T. *Chem. Commun.* **2000**, 1033.
(19) Sasaki, M.; Manseki, K.; Horiuchi, H.; Kumagai, M.; Sakamoto, M.; Sakiyama, H.; Nishida, Y.; Saka, M.; Sadaoka, Y.; Ohba, M.; Okawa, H. *J. Chem. Soc., Dalton Trans.* **2000**, 259.
(20) Goodgame, D. M. L.; Menzer, S.; Ross, A. T.; Williams, D. J. *J. Chem. Soc., Chem. Commun.* **1994**, 2605.
(21) (a) Liu, J.; Meyers, E. A.; Cowan, J. A.; Shore, S. G. *Chem. Commun.* **1998**, 2043. (b) Mao, J.-G.; Song, L.; Huang, J.-S. *Chin, J. Struct. Chem.* **1999**, *18*, 4.
(22) Decurtins, S.; Gross, M.; Schmalle, H. W.; Ferlay, S. *Inorg. Chem.* **1998**, *37*, 2443.

10.1021/ic0100929 CCC: $20.00
Published on Web 08/03/2001

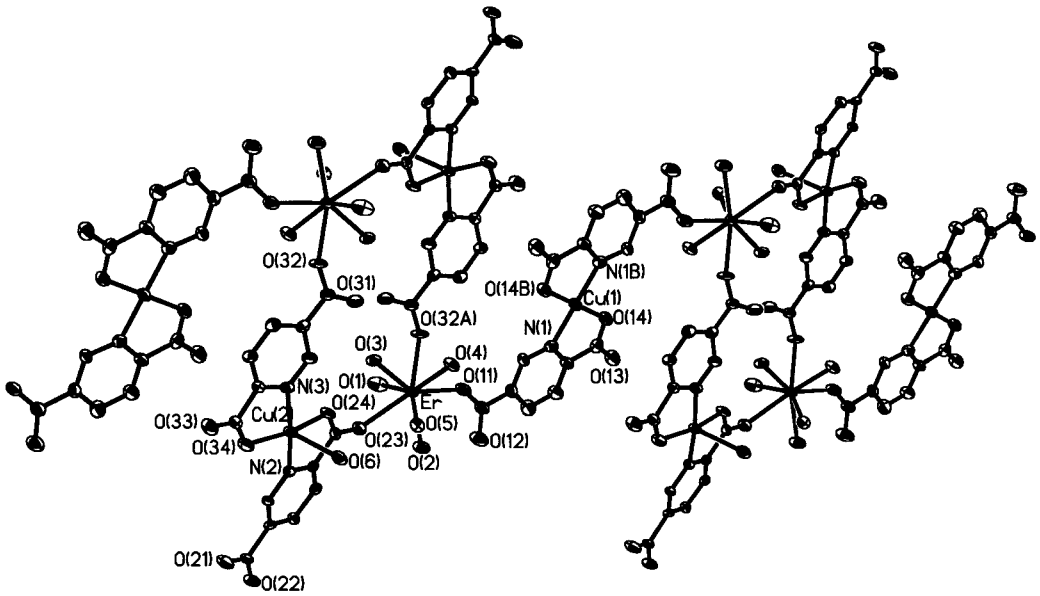

Figure 1. 1-D structure of complex **1** with the atomic labeling scheme. (Thermal ellipsoids are shown at 50% probability.)

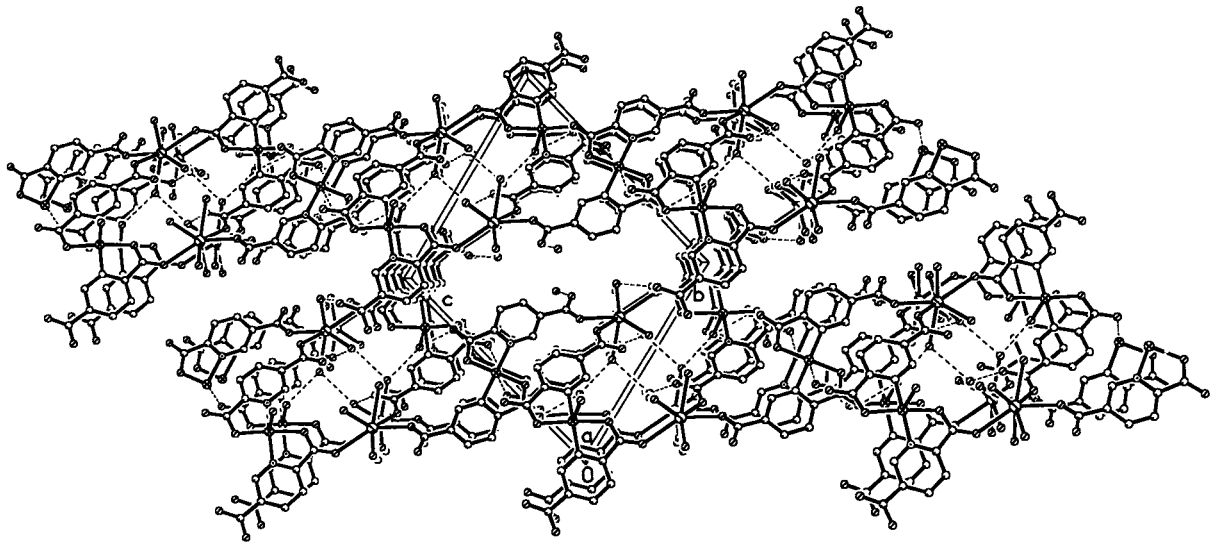

Figure 2. Packing structure along the *a* axis of **1**.

especially Cu(II)−Ln(III) polymeric complexes,[9b,25] are still limited as compared to those of discrete ones. Recently, we have begun studies to use organic ligands for designing magnetic complexes or coordination polymers comprising lanthanide and transition metal ions, especially the Ln−Cu couple, with infinite structures, and hope to provide useful information for the modeling of the magnetic exchange in magnetic materials or novel structure types. After introducing the hydrothermal reaction method in our work, we have successfully isolated two Cu(II)−Gd(III) polymeric complexes constructed by pyridine-2,5-dicarboxylate (pydc).[26] To extend our work, systematic studies have been carried out by employing variable initial reagents of lanthanide(III) and copper(II) along with different reaction conditions. Herein we reported the details of the syntheses and crystal structures of a series of Cu(II)−Ln(III) polymeric complexes, $[\{Ln_2Cu_3(pydc)_6(H_2O)_{12}\}\cdot 4H_2O]_n$ (Ln = Er (**1**); Gd (**2**)), $[\{Ln_4Cu_2(pydc)_8(H_2O)_{12}\}\cdot 4H_2O]_n$ (Ln = Sm (**3**); Gd (**4**); Er (**5**)), and $[Gd_2Cu_2(pydc)_4(H_2O)_8\cdot Cu(pydc)_2\cdot 12H_2O]_n$ (**6**), in which compounds **2** and **4** were recently reported in

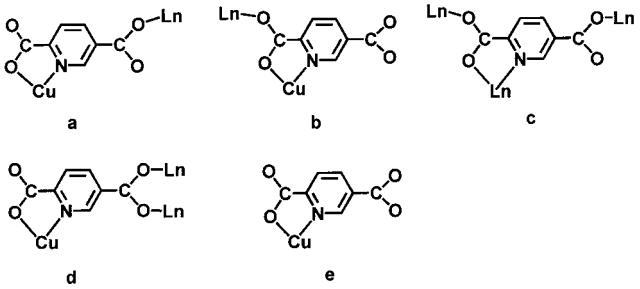

Figure 3. Coordination mode of the pydc ligand.

(23) (a) Jin, T.-Z.; Zhao, S.-F.; Xu, G.-X.; Han, Y.-Z.; Shi, N.-C.; Ma, J.-S. *Acta Chim. Sin.* **1991**, *49*, 569. (b) Goodgame, D. M. L.; Williams, D. J.; Winpenny, R. E. P. *J. Chem. Soc., Dalton Trans.* **1989**, 1439.

(24) Freedman, D.; Kornienko, A.; Emge, T. J.; and Brennan, J. G. *Inorg. Chem.* **2000**, *39*, 2168.

(25) (a)Mao, J.-G.; Song, L.; Huang, J.-S. *J. Chem. Cryst.* **1998**, *28*, 475. (b) Mao, J.-G.; Huang, J.-S.; Ma, J.-F.; Ni, J.-Z. *Transition Met. Chem. (London)* **1997**, *22*, 277. (c) Mao, J.-G.; Song, L.; Huang, X.-Y.; Huang, J.-S. *Polyhedron*. **1997**, *16*, 963. (d) Baggio, R. Garland, M. T. Moreno, Y. Peña, O.; Perec, M.; Spodine, E. *J. Chem. Soc., Dalton Trans*. **2000**, 2061.

(26) Liang, Y. C.; Cao, R.; Su, W. P.; Hong, M. C.; Zhang, W. J. *Angew. Chem., Int. Ed. Engl.* **2000**, *39*, 3304; *Angew. Chem.* **2000**, *39*, 3442.

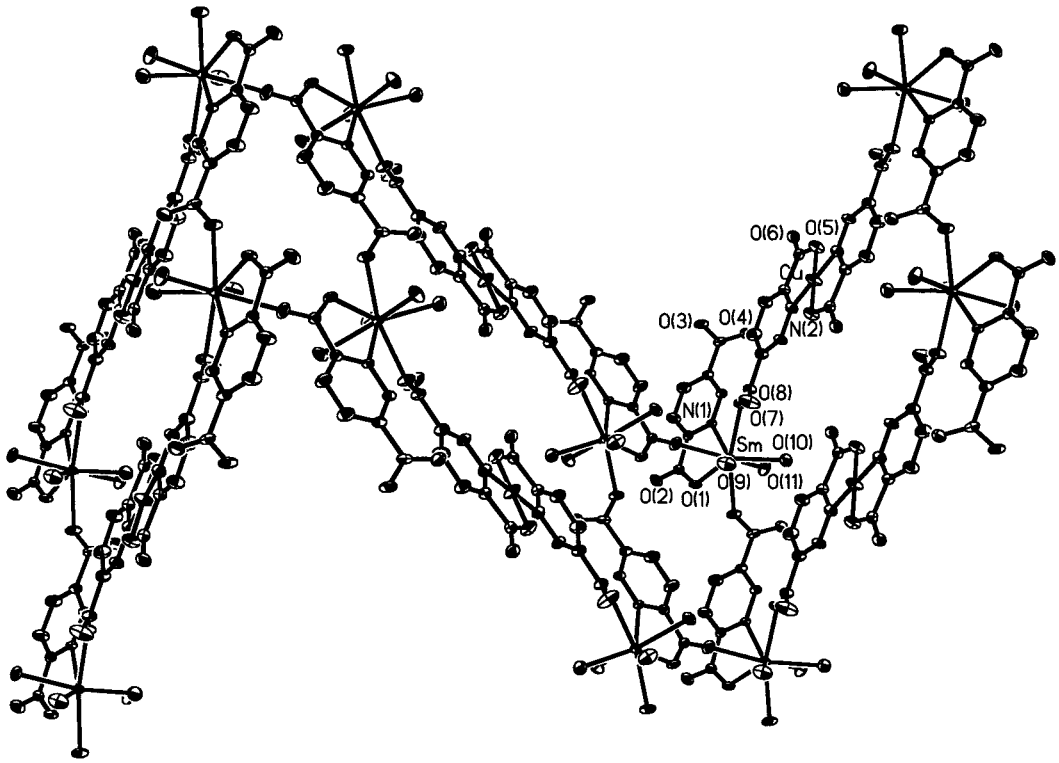

Figure 4. Wavelike structure of **3** with the atomic labeling scheme. (Thermal ellipsoids are shown at 50% probability, and a double zigzag chain is shown for clarity.)

brief,[26] and the magnetic properties of compounds **2**, **4**, and **5** accompanied by the thermal stabilities of complexes **2** and **4**.

Experimental Section

Materials and Analyses. All reagents were commercially available and used without further purification. Elemental analyses were carried out in this institute.

Magnetic Measurements and Spectroscopy. The magnetic susceptibility data were collected as polycrystalline samples at an external field of 1 kG for compounds **2** and **4** and 10 kG for compound **5** on a Quantum Design PPMS model 6000 magnetometer in the temperature range from 5 to 300 K. The output data were corrected for experimentally determined diamagnetism of the sample holder and the diamagnetism of the samples calculated from Pascal's constants. The IR spectra were recorded on a Magna750 FT-IR spectrophotometer using the KBr pellet technique. Thermal gravimetric analysis was performed on a Delta Series TGA7 instrument.

Preparation of Coordination Polymers. [{$Er_2Cu_3(pydc)_6(H_2O)_{12}$}·$4H_2O$]$_n$ (1). The mixture of Er_2O_3 (0.096 g, 0.25 mmol), CuO (0.040 g, 0.5 mmol), pyridine-2,5-dicarboxylic acid (0.167 g, 1.0 mmol), and H_2O (14.0 mL) in the mole ratio of ca. 1:2:4:290 was sealed in a 25 mL stainless steel reactor with Teflon liner and directly heated to 130 °C, kept at 130 °C for 96 h, and then slowly cooled to 30 °C at a rate of 1.39 °C/h. Green-blue crystals of **1** were obtained in 30% yield. Anal. Calcd for $C_{42}H_{50}Cu_3Er_2N_6O_{40}$: C, 27.96; H, 2.79; N, 4.66. Found: C, 28.06; H, 2.73; N, 4.62. IR data (KBr pellet, ν/cm^{-1}): 3386 vs br, 1612 vs, 1390 s, 1358 s, 1284 m, 1036 m, 768 s, 517 m.

[{$Gd_2Cu_3(pydc)_6(H_2O)_{12}$}·$4H_2O$]$_n$ (2). Heating a mixture of Gd_2O_3 (0.090 g, 0.25 mmol), $Cu(OAc)_2$·$2H_2O$ (0.100 g, 0.5 mmol), pyridine-2,5-dicarboxylic acid (0.167 g, 1.0 mmol), and H_2O (14.0 mL) in the mole ratio of ca. 1:2:4:290 in a 25 mL stainless steel reactor with a Teflon liner at 140 °C for 72 h resulted in green-blue crystals of **2**. Yield: 20%. Anal. Calcd for $C_{42}H_{50}Cu_3Gd_2N_6O_{40}$: C, 28.28; H, 2.82; N, 4.71. Found: C, 28.54; H, 2.80; N, 4.74. IR data (KBr pellet, ν/cm^{-1}): 3385 vs br, 1612 vs, 1391 s, 1358 s, 1284 m, 1038 m, 768 s, 517 m.

[{$Sm_4Cu_2(pydc)_8(H_2O)_{12}$}·$4H_2O$]$_n$ (3). Method 1. Heating a mixture of Sm_2O_3 (0.087 g, 0.25 mmol), CuO (0.040 g, 0.50 mmol), pyridine-2,5-dicarboxylic acid (0.167 g, 1.0 mmol), and H_2O (14.0 mL) in the mole ratio of ca. 1:2:4:290 in a 25 mL stainless steel reactor with a Teflon liner at 140 °C for 72 h resulted in blue crystals of **3**. Yield: 25%. Anal. Calcd for $C_{56}H_{56}Cu_2N_8O_{48}Sm_4$: C, 28.77; H, 2.41; N, 4.79. Found: C, 28.75; H, 2.45; N, 4.77. IR data (KBr pellet, ν/cm^{-1}): 3385 vs, br, 1613 vs, 1390 s, 1358 s, 1286 m, 1038 m, 766 s, 514 m.

Method 2. Heating a mixture of Sm_2O_3 (0.087 g, 0.25 mmol), $CuCl_2$·$2H_2O$ (0.085 g, 0.50 mmol), pyridine-2,5-dicarboxylic acid (0.167 g, 1.0 mmol), 2,2′-bipyridine (0.078 g, 0.5 mmol), and H_2O (14.0 mL) in the mole ratio of ca. 1:2:4:2:290 in a 25 mL stainless steel reactor with a Teflon liner at 160 °C for 72 h resulted in blue crystals of **3**. Yield: 75%.

[{$Gd_4Cu_2(pydc)_8(H_2O)_{12}$}·$4H_2O$]$_n$ (4). Method 1. The preparation process is similar to that of compound **3,** except replacing Sm_2O_3 by Gd_2O_3. Heating a mixture of Gd_2O_3 (0.090 g, 0.25 mmol), CuO (0.040 g, 0.50 mmol), pyridine-2,5-dicarboxylic acid (0.167 g, 1.0 mmol), and H_2O (14.0 mL) in the mole ratio of ca. 1:2:4:290 in a 25 mL stainless steel reactor with a Teflon liner at 140 °C for 72 h resulted in blue crystals of **4**. Yield: 75%. Anal. Calcd for $C_{56}H_{56}Cu_2Gd_4N_8O_{48}$: C, 28.44; H, 2.39; N, 4.74. Found: C, 29.14; H, 2.47; N, 4.95. IR data (KBr pellet, ν/cm^{-1}): 3385 vs br, 1610 vs, 1392 s, 1358 s, 1286 m, 1038 m, 766 s, 513 m.

Method 2. Heating a mixture of Gd_2O_3 (0.090 g, 0.25 mmol), $CuCl_2$·$2H_2O$ (0.085 g, 0.50 mmol), pyridine-2,5-dicarboxylic acid (0.167 g, 1.0 mmol), 2,2′-bipyridine (0.078 g, 0.5 mmol), and H_2O (14.0 mL) in the mole ratio of ca. 1:2:4:2:290 in a 25 mL stainless steel reactor with a Teflon liner at 160 °C for 72 h resulted in blue crystals of **4**. Yield: 81%.

[{$Er_4Cu_2(pydc)_8(H_2O)_{12}$}·$4H_2O$]$_n$ (5). Heating a mixture of Er_2O_3 (0.096 g, 0.25 mmol), $CuCl_2$·$2H_2O$(0.085 g, 0.50 mmol), pyridine-2,5-dicarboxylic acid (0.167 g, 1.0 mmol), 2,2′-bipyridine (0.078 g, 0.50 mmol), and H_2O (12.0 mL) in a 25 mL stainless steel reactor with a Teflon liner at 160 °C for 29 h resulted in blue crystals of **5**. Yield: 75%. Anal. Calcd for $C_{56}H_{56}Cu_2Er_4N_8O_{48}$: C, 27.96; H, 2.35; N, 4.66. Found: C, 28.16; H, 2.24; N, 4.68. IR data (KBr pellet, ν/cm^{-1}): 3388 vs br, 1608 vs, 1387 s, 1360 s, 1286 m, 1038 m, 766 s, 515 m.

[$Gd_2Cu_2(pydc)_4(H_2O)_8$·$Cu(pydc)_2$·$12H_2O$]$_n$ (6). The mixture of Gd_2O_3 (0.090 g, 0.25 mmol), $Cu(OAc)_2$·$2H_2O$ (0.100 g, 0.5 mmol),

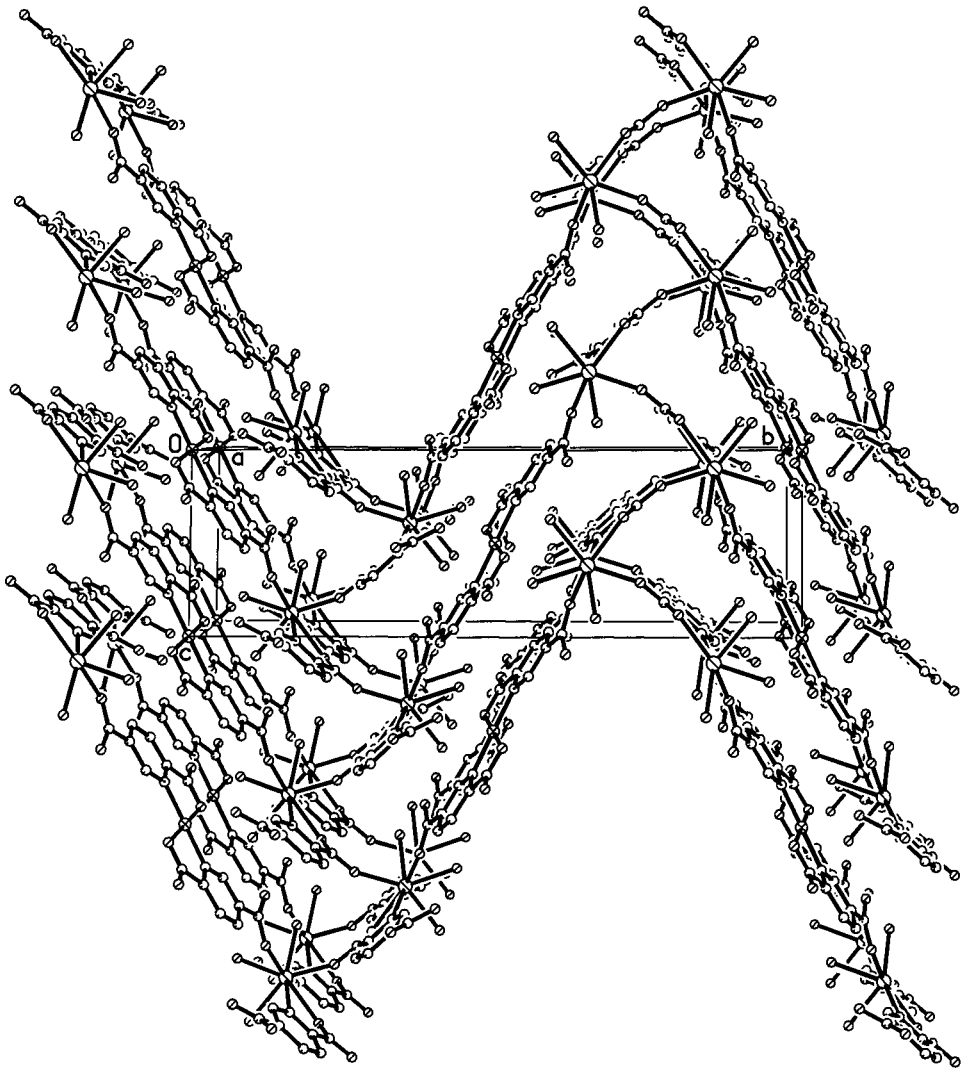

Figure 5. Packing structure along the *a* axis of **3**.

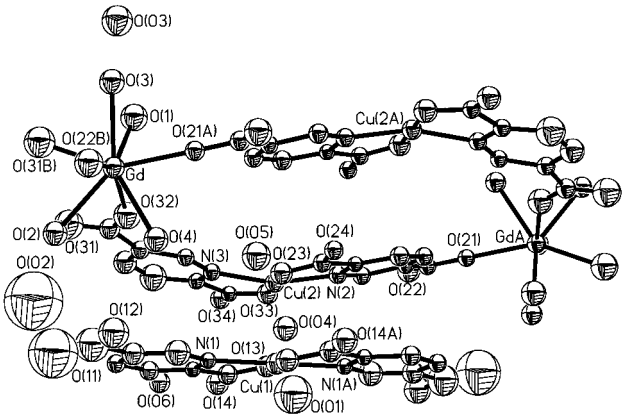

Figure 6. Basic unit structure of compound **6** with the atomic labeling scheme. (Thermal ellipsoids are shown at 30% probability.)

pyridine-2,5-dicarboxylic acid (0.167 g, 1.0 mmol), and H_2O (14.0 mL) in the mole ratio of ca. 1:2:4:290 was sealed in a 25 mL stainless steel reactor with a Teflon liner and slowly heated to 140 °C from room temperature at a rate of 1.60 °C/h, kept at 140 °C for 96 h, and then slowly cooled to 30 °C at the rate of 1.60 °C/h. The purple-blue crystals of **6** were obtained in yield 20%. Anal. Calcd for $C_{42}H_{58}Cu_3Gd_2N_6O_{44}$: C, 27.18; H, 3.15; N, 4.53. Found: C, 27.29; H, 3.07; N, 4.59. IR data (KBr pellet, ν/cm^{-1}): 3385 vs, br, 1611 vs, 1390 s, 1358 s, 1284 m, 1038 m, 768 s, 516 m.

Single-Crystal X-ray Structure Determination. The crystal data and data collection parameters for **1**−**6** are summarized in Table 1. Selected bond lengths and bond angles of compounds **1**−**6** are given in Tables 2−4. The intensity data for **1**−**6** were collected on a SIEMENS SMART CCD diffractometer with graphite-monochromated Mo Kα (λ = 0.710 73 Å) radiation in the $\omega-2\theta$ scanning mode at room temperature. The data were corrected for Lorentz and polarization effects as well as absorption. All structures were solved by direct methods. The heavy atoms were located from the *E*-maps; other non-hydrogen atoms were derived from the successive difference Fourier syntheses. The structure was refined on F^2 by full-matrix least-squares methods using the SHELXTL-97 program package on a legend 586 computer. All non-hydrogen atoms were refined anisotropically.

Results and Discussion

Syntheses. The hydrothermal reactions of lanthanide oxide, pyridine-2,5-dicarboxylic acid, and copper(II) oxide or copper-(II) salts resulted in the formation of complexes **1**−**6**. It is interesting that although the molar ratios of lanthanide(III) and copper(II) reagents in the syntheses are the same, the different forms of Cu(II) and the crystal growth conditions remarkably influence the Cu/Ln ratios, the structures, the coordination environments of the metal centers, and coordination modes of pydc ligands in the products thus formed. For the reactions of $Cu(OAc)_2$, copper(II) ions are readily coordinated to nitrogen atoms of pydc ligands; thus, all nitrogens are coordinated by copper(II) giving rise to high Cu/Ln ratio (3/2) products **1**, **2**,

Table 1. Crystal Data for **1**−**6**

param	**1**	**2**	**3**	**4**	**5**	**6**
formula	$C_{42}H_{50}Cu_3Er_2N_6O_{40}$	$C_{42}H_{50}Cu_3Gd_2N_6O_{40}$	$C_{56}H_{56}Cu_2N_8O_{48}Sm_4$	$C_{56}H_{56}Cu_2Gd_4N_8O_{48}$	$C_{56}H_{56}Cu_2Er_4N_8O_{48}$	$C_{42}H_{58}Cu_3Gd_2N_6O_{44}$
fw	1804.02	1784.00	2337.57	2365.17	2405.21	1856.06
space group	$P\bar{1}$	$P\bar{1}$	$P2_1/c$	$P2_1/c$	$P2_1/c$	$P\bar{1}$
a, Å	7.3601(3)	9.393(2)	9.296(3))	9.260(2)	9.1721(5)	10.1194(6)
b, Å	13.5424(5)	13.567(6)	25.562(5)	25.543(5)	25.4000(15)	10.5763(5)
c, Å	15.1256(5)	15.169(4)	7.8110(15)	7.7815(13)	7.7385(4)	14.3500(8)
α, deg	72.5820(10)	72.62(2)	90	90	90	95.333(2)
β, deg	76.2630(10)	76.15(2)	97.27(2)	97.36(2)	97.3390(10)	101.675(2)
γ, deg	80.1520(10)	80.17(3)	90	90	90	105.61
V, Å^3	1389.20(9)	1401.7(7)	1841.2(8)	1825.3(6)	1788.08(17)	1430.80(13)
Z	1	1	1	1	1	1
ρ_{calcd}, g cm^{-3}	2.156	2.113	2.108	2.152	2.234	2.154
μ, mm^{-1}	4.238	3.572	3.821	4.271	5.344	3.509
Temp, K	293(2)	293(2)	293(2)	293(2)	293(2)	293(2)
λ(Mo Kα), Å	0.710 73	0.710 73	0.710 73	0.710 73	0.710 73	0.710 73
R1[$I > 2\sigma(I)$][a]	0.0416	0.0426	0.0332	0.0341	0.0419	0.0873
R_w [$I > 2\sigma(I)$][b]	0.0994	0.0973	0.0789	0.0882	0.1044	0.2032

[a] $R = \Sigma||F_o| - |F_{cl}|)/\Sigma|F_o|$. [b] $R_w = [\Sigma w(F_o^2 - F_c^2)^2]/\Sigma|wF_o|^2]^{1/2}$.

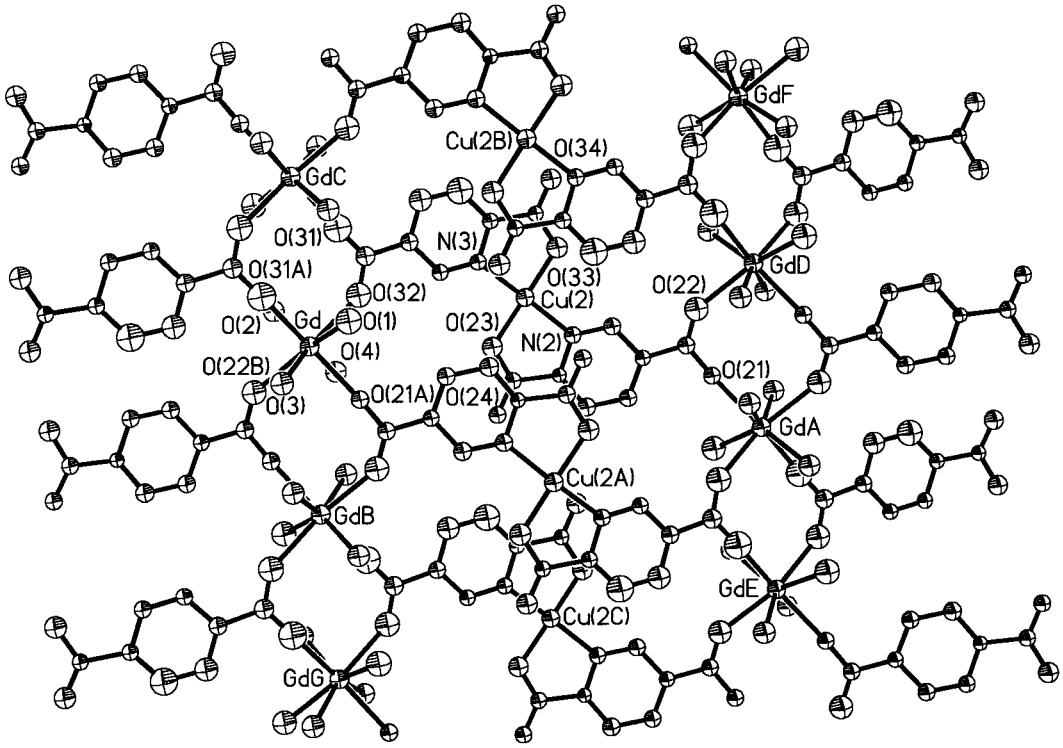

Figure 7. 2D structure of $[Gd_2Cu_2(pydc)_4(H_2O)_8]^{2+}$ in compound **6** with the atomic labeling scheme. (Thermal ellipsoids are shown at 30% probability.)

and **6**. However, if CuO is used as a reagent, the reaction rate of CuO may be comparable with that of Ln_2O_3 and the nitrogen atoms are bound simultaneously by Ln(III) and Cu(II), inducing low Cu/Ln ratio (1/2) products **3** and **4**. To confirm this speculation, $CuCl_2{\cdot}2H_2O$ was employed in the synthetic reactions, with the presence of auxiliary ligand 2,2′-bipyridine. As expected, low Cu/Ln ratio complexes **3**−**5** were obtained in high yield because 2,2′-bipyridine may easily coordinate to Cu(II) ions and can be replaced by pydc as the reactions proceed, preventing all nitrogen atoms of pydc ligands from coordinating to Cu(II) ions and resulting in a low Cu/Ln ratio; the high yields may be ascribed to the protection of quick polymerization by 2,2′-bipyridine. The formation of **6** may be due to the different crystal growth conditions, but detailed elucidation still remains unclear.

Thermogravimetric Analyses. Owing to the similarity of the structures for the six complexes, **2** and **4** were selected for thermogravimetric (TG) analyses, to examine the thermal stability of complexes. The TGA curve for **2** displays that the first weight loss of 10.562% between 50 and 131.57 °C corresponds to the loss of four uncoordinated discrete water molecules and six coordination waters (calculated: 10.09%), and the second weight loss of 5.52% between 131.57 and 277.44 °C corresponds to the loss of six coordinated water molecules (calculated: 6.06%). The total of two step loss weight is 16.08%; it equates to the loss of all coordinated water and uncoordinated water (calculated: 16.16%). Then decomposition of compound **2** started above 277.44 °C. The TGA curve for **4** shows that the first weight loss of 2.311% between 50 and 110.97 °C corresponds to the loss of the uncoordinated discrete water molecules (calculated: 3.05%) and the second weight loss of 9.159% between 110.97 and 298 °C corresponds to the loss of the coordinated water molecules (calculated: 9.14%); the total loss of weight of the two steps of 11.82% corresponds to the

Table 2. Selected Bond Lengths (Å) and Bond Angles (deg) for Compounds **1** and **2**

		1	
Er−O(11)	2.304(5)	Cu(1)−O(14)	1.929(5)
Er−O(2)	2.310(5)	Cu(1)−N(1B)	1.968(6)
Er−O(3)	2.313(5)	Cu(1)−N(1)	1.968(6)
Er−O(1)	2.335(6)	Cu(2)−O(34)	1.933(5)
Er−O(32A)	2.386(5)	Cu(2)−N(3)	1.945(6)
Er−O(4)	2.398(5)	Cu(2)−O(24)	1.967(5)
Er−O(5)	2.433(5)	Cu(2)−N(2)	1.971(6)
Er−O(23)	2.454(5)	Cu(2)−O(6)	2.373(5)
		Cu(1)−O(14B)	1.929(5)
O(11)−Er−O(2)	74.70(19)	O(2)−Er−O(23)	68.67(18)
O(11)−Er−O(3)	144.08(19)	O(3)−Er−O(23)	74.27(18)
O(2)−Er−O(3)	140.69(19)	O(1)−Er−O(23)	72.0(2)
O(11)−Er−O(1)	94.9(2)	O(32A)−ErO(23)	132.00(19)
O(2)−Er−O(1)	87.9(2)	O(4)−Er−O(23)	133.90(18)
O(3)−Er−O(1)	92.9(2)	O(5)−Er−O(23)	72.17(18)
O(11)−Er−O(32A)	73.04(19)	O(14B)−Cu(1)−O(14)	180.0(3)
O(2)−Er−O(32A)	140.5(2)	O(14B)−Cu(1)−N(1B)	84.2(2)
O(3)−Er−O(32A)	75.95(18)	O(14)−Cu(1)−N(1B)	95.8(2)
O(1)−Er−O(32A)	72.9(2)	O(14B)−Cu(1)−N(1)	95.8(2)
O(11)−Er−O(4)	76.1(2)	O(14)−Cu(1)−N(1)	84.2(2)
O(2)−Er−O(4)	120.1(2)	N(1B)−Cu(1)−N(1)	180.000(2)
O(3)−Er−O(4)	77.77(19)	O(34)−Cu(2)−N(3)	83.5(2)
O(1)−Er−O(4)	145.7(2)	O(34)−Cu(2)−O(24)	167.9(2)
O(32A)−Er−O(4)	72.86(19)	N(3)−Cu(2)−O(24)	94.2(2)
O(11)−Er−O(5)	111.3(2)	O(34)−Cu(2)−N(2)	97.4(2)
O(2)−Er−O(5)	76.5(2)	N(3)−Cu(2)−N(2)	170.1(3)
O(3)−Er−O(5)	80.25(18)	O(24)−Cu(2)−N(2)	82.9(2)
O(1)−Er−O(5)	144.00(19)	O(34)−Cu(2)−O(6)	106.1(2)
O(32A)−Er−O(5)	137.08(18)	N(3)−Cu(2)−O(6)	96.2(2)
O(4)−Er−O(5)	67.48(18)	O(24)−Cu(2)−O(6)	85.9(2)
O(11)−Er−O(23)	141.25(18)	N(2)−Cu(2)−O(6)	93.1(2)
		2	
Gd−O(11)	2.329(5)	Cu(1)−O(14B)	1.936(5)
Gd−O(3)	2.367(5)	Cu(1)−N(1)	1.970(6)
Gd−O(2)	2.368(5)	Cu(1)−N(1B)	1.970(6)
Gd−O(1)	2.390(6)	Cu(2)−O(34)	1.931(5)
Gd−O(32A)	2.416(5)	Cu(2)−N(3)	1.951(6)
Gd−O(4)	2.446(5)	Cu(2)−O(24)	1.966(5)
Gd−O(23)	2.480(5)	Cu(2)−N(2)	1.973(5)
Gd−O(5)	2.490(5)	Cu(2)−O(6)	2.381(6)
		Cu(1)−O(14)	1.936(5)
O(11)−Gd−O(3)	143.7(2)	O(1)−Gd−O(32A)	73.4(2)
O(11)−Gd−O(2)	74.0(2)	O(11)−Gd−O(4)	76.8(2)
O(3)−Gd−O(2)	141.4(2)	O(3)−Gd−O(4)	76.1(2)
O(11)−Gd−O(1)	97.4(2)	O(2)−Gd−O(4)	120.3(2)
O(3)−Gd−O(1)	91.6(2)	O(1)−Gd−O(4)	145.8(2)
O(2)−Gd−O(1)	89.2(2)	O(32A)−Gd−O(4)	72.6(2)
O(11)−Gd−O(32A)	73.2(2)	O(11)−Gd−O(23)	141.7(2)
O(3)−Gd−O(32A)	76.0(2)	O(3)−Gd−O(23)	74.4(2)
O(2)−Gd−O(32A)	140.2(2)	O(2)−Gd−O(23)	69.4(2)
O(1)−Gd−O(23)	71.7(2)	O(14)−Cu(1)−N(1B)	95.9(2)
O(32A)−Gd−O(23)	132.9(2)	O(14B)−Cu(1)−N(1B)	84.1(2)
O(4)−Gd−O(23)	132.1(2)	N(1)−Cu(1)−N(1B)	180.000(2)
O(11)−Gd−O(5)	110.1(2)	O(34)−Cu(2)−N(3)	83.3(2)
O(3)−Gd−O(5)	80.3(2)	O(34)−Cu(2)−O(24)	167.9(2)
O(2)−Gd−O(5)	76.5(2)	N(3)−Cu(2)−O(24)	94.5(2)
O(1)−Gd−O(5)	143.6(2)	O(34)−Cu(2)−N(2)	97.4(2)
O(32A)−Gd−O(5)	136.5(2)	N(3)−Cu(2)−N(2)	170.2(2)
O(4)−Gd−O(5)	66.6(2)	O(24)−Cu(2)−N(2)	82.8(2)
O(23)−Gd−O(5)	71.9(2)	O(34)−Cu(2)−O(6)	106.0(2)
O(14)−Cu(1)−O(14B)	180.000(1)	N(3)−Cu(2)−O(6)	96.7(2)
O(14)−Cu(1)−N(1)	84.1(2)	O(24)−Cu(2)−O(6)	86.1(2)
O(14B)−Cu(1)−N(1)	95.9(2)	N(2)−Cu(2)−O(6)	92.5(2)

loss of all discrete water and coordinated water molecules (calculated: 12.18%), and then decomposition of compound **4** started above 298 °C.

Structure Description. The crystal structures for **2** and **4** have been reported previously[26] and will not be described herein.

[{$Er_2Cu_3(pydc)_6(H_2O)_{12}$}·$4H_2O$]$_n$ (1). Compound **1** is isomorphous to the previous reported complex **2** (see Table 2) and also displays a one-dimensional (1-D) chain structure. As shown in Figure 1, the chain consists of two building blocks, [Er_2Cu_2(pydc)$_4$(H_2O)$_{12}$] and [Cu(pydc)$_2$], which are linked to each other by pydc ligands through Er−O bonds. There are two types of environments around the Cu(II) atoms: Cu(1) atom in [Cu(pydc)$_2$] is chelated by two pydc ligands through nitrogen and oxygen atoms in an exactly square planar geometry [Cu(1)−O(14) = 1.929(5) and Cu(1)−N(1) = 1.968(6) Å]. The bond angles of N(1)−Cu(1)−O(14), N(1)−Cu(1)−N(1B), N(1)−Cu(1)−O(14B), and O(14)−Cu(1)−O(14B) are 84.2(2), 180.000(2), 95.8(2), and 180.000(1)°, respectively. The Cu(2) atom in [Er_2Cu_2(pydc)$_4$(H_2O)$_{12}$] is coordinated by two nitrogen and two oxygen atoms from two pydc ligands and one oxygen atom from a coordinated water molecule in a distorted square-pyramid geometry, in which the four donor atoms from pydc (O(24), O(34), N(2), and N(3)) make up of the basal plane and one oxygen from water (O(6)) occupies the apex, with the bond angles of O(6)−Cu(2)−O(24, 34) and O(6)−Cu(2)−N(2, 3) ranging from 85.9(2) to 106.1(2)° and from 93.1(2) to 96.2(2)°, respectively. O(24)−Cu(2)−O(34) and N(3)−Cu(2)−N(2) are 167.9(2) and 170.1(3)°, respectively. The Cu−O_{pydc} and Cu−N bonds show typical lengths (Cu(2)−O(34) 1.933(5), Cu(2)−O(24) 1.967(5), Cu(2)−N(3) 1.945(6), and Cu(2)−N(4) 1.971(6) Å), while the Cu(2)−O(6) distance (2.373(5) Å) is rather long, indicating that the Cu−O_{water} bond is weak. Every europium(III) center is coordinated by eight oxygen atoms, three from pydc and five from coordinated water molecules with the Er−O distances ranging from 2.304(5) to 2.454(5) Å and O−Er−O bond angle falling in the range of 67.48(18)−145.7(2)°. Two types of pydc ligands are present in **1**; one adopts the tridentate chelating-bridging coordination mode through a long bridge via a pyridyl ring, linking one copper(II) and one europium(III) center (Figure 3a), and the other adopts a tridentate chelating-bridging mode through a short bridge via a carboxylate group neighboring the nitrogen atom, also linking one copper(II) and one europium(III) center (Figure 3b). The chain can also be viewed as two building blocks [Cu(pydc)$_2$] and [Cu(pydc)$_2$(H_2O)], connected by europium(III) linkers, in which each europium(III) linker connects one [Cu(pydc)$_2$] and two [Cu(pydc)$_2$(H_2O)] units. The 1-D chains are linked by the hydrogen bonds to form layer structures which are further linked by the hydrogen bonds to form a three-dimensional structure (Figure 2). Europium to europium, europium to copper, and copper to copper distances between the adjacent units are 6.208, 5.771, and 5.093 Å, respectively, indicating no existence of directe M−M interactions.

[{$Sm_4Cu_2(pydc)_8(H_2O)_{12}$}·$4H_2O$]$_n$ (3). Compound **3** is isomorphous to **4** (see Table 3) and displays a 3-D wavelike polymeric structure consisting of [Sm_4Cu_2(pydc)$_8$(H_2O)$_{12}$] basic units, which are linked head to tail to form infinite zigzag chains via Sm−O_{pydc} bonding (Figure 4). Each of two neighboring chains are linked together to generate wavelike two-dimensional (2-D) structures, which are further connected to each other by pydc ligands to produce the 3-D structure, as shown in Figure 5. The 2-D wave can also be viewed as Sm−Cu ladders in which the rungs are formed by [Cu(pydc)$_2$] species and the side pieces by samarium(III) chains; the side pieces of the neighboring ladders are linked by pydc via Sm−O bonds to yield the wave. Each copper(II) is chelated by two pydc groups through nitrogen and oxygen atoms in an exactly square planar geometry (both O(5)−Cu−O(5B) and N(2)−Cu−N(2B) bond angle are 180.00°). The Cu−N(2) and Cu−O(5) bonds are 1.965(5) and 1.945(4) Å, similar to those in **1**. Each samarium(III) center is coordinated by one nitrogen and four oxygen atoms from four pydc ligands and three oxygen atoms from coordinated water molecules with

Table 3. Selected Bond Lengths (Å) and Bond Angles (deg) for Compounds **3**−**5**

3			
Sm−O(3D)	2.352(4)	Sm−O(9)	2.462(4)
Sm−O(2A)	2.353(4)	Sm−N(1)	2.599(5)
Sm−O(7)	2.405(4)	Cu−O(5)	1.945(4)
Sm−O(11)	2.424(4)	Cu−O(5B)	1.945(4)
Sm−O(1)	2.432(4)	Cu−N(2)	1.965(5)
Sm−O(10)	2.436(4)	Cu−N(2B)	1.965(5)
O(3D)−Sm−O(2A)	107.81(15)	O(7)−Sm−O(9)	79.47(14)
O(3D)−Sm−O(7)	149.11(14)	O(11)−Sm−O(9)	142.79(16)
O(2A)−Sm−O(7)	82.90(15)	O(1)−Sm−O(9)	127.55(15)
O(3D)−Sm−O(11)	85.67(15)	O(10)−Sm−O(9)	73.78(16)
O(2A)−Sm−O(11)	139.68(15)	O(3D)−Sm−N(1)	136.43(14)
O(7)−Sm−O(11)	105.03(14)	O(2A)−Sm−N(1)	73.58(14)
O(3D)−Sm−O(1)	75.12(13)	O(7)−Sm−N(1)	74.06(14)
O(2A)−Sm−O(1)	72.23(15)	O(11)−Sm−N(1)	71.05(14)
O(7)−Sm−O(1)	135.36(13)	O(1)−Sm−N(1)	63.73(13)
O(11)−Sm−O(1)	75.18(14)	O(10)−Sm−N(1)	123.26(15)
O(3D)−Sm−O(10)	80.10(15)	O(9)−Sm−N(1)	142.50(15)
O(2A)−Sm−O(10)	146.77(16)	O(5)−Cu−O(5B)	180.000(1)
O(7)−Sm−O(10)	76.18(14)	O(5)−Cu−N(2)	83.77(18)
O(11)−Sm−O(10)	71.69(15)	O(5B)−Cu−N(2)	96.23(18)
O(1)−Sm−O(10)	139.71(14)	O(5)−Cu−N(2B)	96.23(18)
O(3D)−Sm−O(9)	75.08(15)	O(5B)−Cu−N(2B)	83.77(18)
O(2A)−Sm−O(9)	77.24(16)	N(2)−Cu−N(2B)	180.000(2)
4			
Gd−O(3D)	2.335(4)	Gd−O(9)	2.434(4)
Gd−O(2A)	2.338(4)	Gd−N(1)	2.575(4)
Gd−O(7)	2.372(3)	Cu−O(5B)	1.946(4)
Gd−O(11)	2.397(4)	Cu−O(5)	1.946(4)
Gd−O(10)	2.404(4)	Cu−N(2)	1.970(4)
Gd−O(1)	2.415(4)	Cu−N(2B)	1.970(4)
O(3D)−Gd−O(2A)	106.83(14)	O(3D)−Gd−O(1)	74.14(13)
O(3D)−Gd−O(7)	149.54(13)	O(2A)−Gd−O(1)	72.28(14)
O(2A)−Gd−O(7)	83.34(14)	O(7)−Gd−O(1)	135.87(12)
O(3D)−Gd−O(11)	85.93(14)	O(11)−Gd−O(1)	75.60(14)
O(2A)−Gd−O(11)	140.21(14)	O(10)−Gd−O(1)	139.58(14)
O(7)−Gd−O(11)	104.74(14)	O(3D)−Gd−O(9)	74.58(14)
O(3D)−Gd−O(10)	80.61(14)	O(2A)−Gd−O(9)	76.8(2)
O(2A)−Gd−O(10)	146.6(2)	O(7)−Gd−O(9)	80.23(14)
O(7)−Gd−O(10)	76.14(14)	O(11)−Gd−O(9)	142.6(2)
O(11)−Gd−O(10)	71.54(14)	O(10)−Gd−O(9)	73.9(2)
O(1)−Gd−O(9)	126.52(14)	O(9)−Gd−N(1)	143.00(14)
O(3D)−Gd−N(1)	136.18(13)	O(5B)−CuO(5)	180.000(1)
O(2A)−Gd−N(1)	74.31(14)	O(5B)-Cu−N(2)	96.2(2)
O(7)−Gd−N(1)	73.92(13)	O(5)−Cu−N(2)	83.8(2)
O(11)−Gd−N(1)	70.96(13)	O(5B)−Cu−N(2B)	83.8(2)
O(10)−Gd−N(1)	123.09(14)	O(5)−Cu−N(2B)	96.2(2)
O(1)−Gd−N(1)	64.45(12)	N(2)−Cu−N(2B)	180.000(2)
5			
Er−O(3D)	2.276(6)	Er−O(9)	2.388(6)
Er−O(2A)	2.279(5)	Er−N(1)	2.526(6)
Er−O(7)	2.329(5)	Cu−O(5B)	1.943(6)
Er−O(11)	2.347(5)	Cu−O(5)	1.943(6)
Er−O(10)	2.357(5)	Cu−N(2)	1.970(6)
Er−O(1)	2.372(5)	Cu−N(2B)	1.970(6)
O(3D)−Er−O(2A)	106.7(2)	O(7)−Er−O(9)	80.44(19)
O(3D)−Er−O(7)	149.41(19)	O(11)−Er−O(9)	142.4(2)
O(2A)−Er−O(7)	83.1(2)	O(10)−Er−O(9)	73.6(2)
O(3D)−Er−O(11)	86.0(2)	O(1)−Er−O(9)	125.5(2)
O(2A)−Er−O(11)	141.1(2)	O(3D)−Er−N(1)	136.71(19)
O(7)−Er−O(11)	104.7(2)	O(2A)−Er−N(1)	75.1(2)
O(3D)−Er−O(10)	80.60(19)	O(7)−Er−N(1)	73.51(18)
O(2A)−Er−O(10)	145.5(2)	O(11)−Er−N(1)	71.09(19)
O(7)−Er−O(10)	76.0(2)	O(10)−Er−N(1)	122.94(19)
O(11)−Er−O(10)	71.8(2)	O(1)−Er−N(1)	65.68(18)
O(3D)−Er−O(1)	73.60(18)	O(9)−Er−N(1)	143.0(2)
O(2A)−Er−O(1)	72.6(2)	O(5B)−Cu−O(5)	180.000(1)
O(7)−Er−O(1)	136.45(18)	O(5B)−Cu−N(2)	96.2(3)
O(11)−Er−O(1)	76.3(2)	O(5)−Cu−N(2)	83.8(3)
O(10)−Er−O(1)	140.0(2)	O(5B)−Cu−N(2B)	83.8(3)
O(3D)−Er−O(9)	74.2(2)	O(5)−Cu−N(2B)	96.2(3)
O(2A)−Er−O(9)	76.1(2)	N(2)−Cu−N(2B)	180.0(3)

Table 4. Selected Bond Lengths (Å) and Bond Angles (deg) for Compound **6**

6			
Gd−O(21A)	2.301(10)	Cu(1)−O(13A)	1.972(11)
Gd−O(31B)	2.303(13)	Cu(1)−O(13)	1.972(11)
Gd−O(22B)	2.342(11)	Cu(1)−N(1)	2.002(14)
Gd−O(32)	2.345(12)	Cu(1)−N(1A)	2.002(14)
Gd−O(2)	2.433(11)	Cu(2)−O(33)	1.911(11)
Gd−O(1)	2.436(14)	Cu(2)−O(23)	1.932(10)
Gd−O(3)	2.439(14)	Cu(2)−N(3)	1.965(13)
Gd−O(4)	2.458(12)	Cu(2)−N(2)	1.970(12)
O(21A)−Gd−O(31B)	148.7(5)	O(2)−Gd−O(1)	134.1(5)
O(21A)−Gd−O(22B)	95.4(4)	O(21A)−Gd−O(3)	77.3(5)
O(31B)−Gd−O(22B)	92.8(4)	O(31B)−Gd−O(3)	76.8(6)
O(21A)-Gd−O(32)	95.6(4)	O(22B)−Gd−O(3)	71.7(5)
O(31B)-Gd−O(32)	94.3(4)	O(32)−Gd−O(3)	142.3(5)
O(22B)−Gd−O(32)	145.9(5)	O(2)−Gd−O(3)	132.2(5)
O(21A)−Gd−O(2)	139.5(5)	O(1)−Gd−O(3)	68.8(5)
O(31B)−Gd−O(2)	71.8(5)	O(21A)−Gd−O(4)	69.6(4)
O(22B)−Gd−O(2)	74.8(4)	O(31B)−Gd−O(4)	141.7(5)
O(32)−Gd−O(2)	75.9(5)	O(22B)−Gd−O(4)	79.0(5)
O(21A)−Gd−O(1)	77.3(5)	O(32)−Gd−O(4)	74.8(5)
O(31B)-Gd−O(1)	77.2(5)	O(2)−Gd−O(4)	70.0(4)
O(22B)−Gd−O(1)	140.5(5)	O(1)−Gd−O(4)	131.0(5)
O(32)−Gd−O(1)	73.5(5)	O(3)−Gd−O(4)	132.9(5)
O(13A)−Cu(1)−O(13)	180.0(6)	O(33)−Cu(2)−O(23)	177.9(5)
O(13A)−Cu(1)−N(1)	97.2(5)	O(33)−Cu(2)−N(3)	85.5(5)
O(13)−Cu(1)−N(1)	82.8(5)	O(23)−Cu(2)−N(3)	94.2(5)
O(13A)−Cu(1)−N(1A)	82.8(5)	O(33)−Cu(2)−N(2)	95.8(5)
O(13)−Cu(1)−N(1A)	97.2(5)	O(23)−Cu(2)−N(2)	85.0(5)
N(1)−Cu(1)−N(1A)	180.0(8)	N(3)−Cu(2)−N(2)	162.9(6)

the Sm−O bonds ranging from 2.352(4) to 2.462(4) Å and the Sm−N bond being 2.599(5) Å. O−Sm−O bond angles range from 71.69(15) to 149.11(14)°, and O−Sm−N bond angles fall in the range of 63.73(13)−142.50(15)°. There are also two types of pydc ligands in **3**; one adopts a tridentate chelating-bridging coordination mode through a long bridge via a pyridyl ring, linking one copper(II) and one samarium(III) center (Figure 3a), the same as that in **1**, and the other adopts a tetradentate chelating-bridging mode through both short and long bridges, linking three samarium(III) centers (Figure 3c). Samarium to samarium, samarium to copper, and copper to copper distances between the adjacent units are 6.418, 6.041, and 7.811 Å, respectively.

$[\{Er_4Cu_2(pydc)_8(H_2O)_{12}\}\cdot 4H_2O]_n$ (5). The crystal structure of **5** is isomorphous to those of **3** and **4** (see Table 3); only very small metric differences have been observed for the three compounds because the radius of a Er(III) ion is slightly smaller than that of Sm(III) ions. Thus all of the metal−ligand bonds in **5** are slightly shorter than the corresponding bonds in **3** and **4**, as compared in Table 3. At the same time, all of bond angles in compound **5** have slight differences compared to the corresponding parameters of complexes **3** and **4**. Er−Er, Er−Cu, and Cu−Cu distances between the adjacent units are 6.340, 6.006, and 7.738 Å, respectively.

$[Gd_2Cu_2(pydc)_4(H_2O)_8\cdot Cu(pydc)_2\cdot 12H_2O]_n$ (6). Compound **6** has a sandwichlike structure (see Table 4) consisting of an infinite lay-like $[Gd_2Cu_2(pydc)_4(H_2O)_8]$ cation and discrete $[Cu(pydc)_2]$ anion units and water molecules, as illustrated in Figure 6. The copper(II) atom in the anion unit is chelated by two pydc ligands through nitrogen and oxygen atoms in an exactly square planar geometry, with Cu(1)−O(13) and Cu(1)−N(1) distances being 1.972(11) and 2.002(14) Å, respectively, and N(1)−Cu(1)−N(1A) and O(13)−Cu(1)−O(13A) angles being 180.0(8) and 180.0(6)°, respectively. In the $[Cu(pydc)_2]^{2-}$ anion, pydc adopts a bidentate-chelating mode through its nitrogen atom and one oxygen atom from the adjacent carboxylate group; another carboxylate group remains free (Figure 3e). However, the

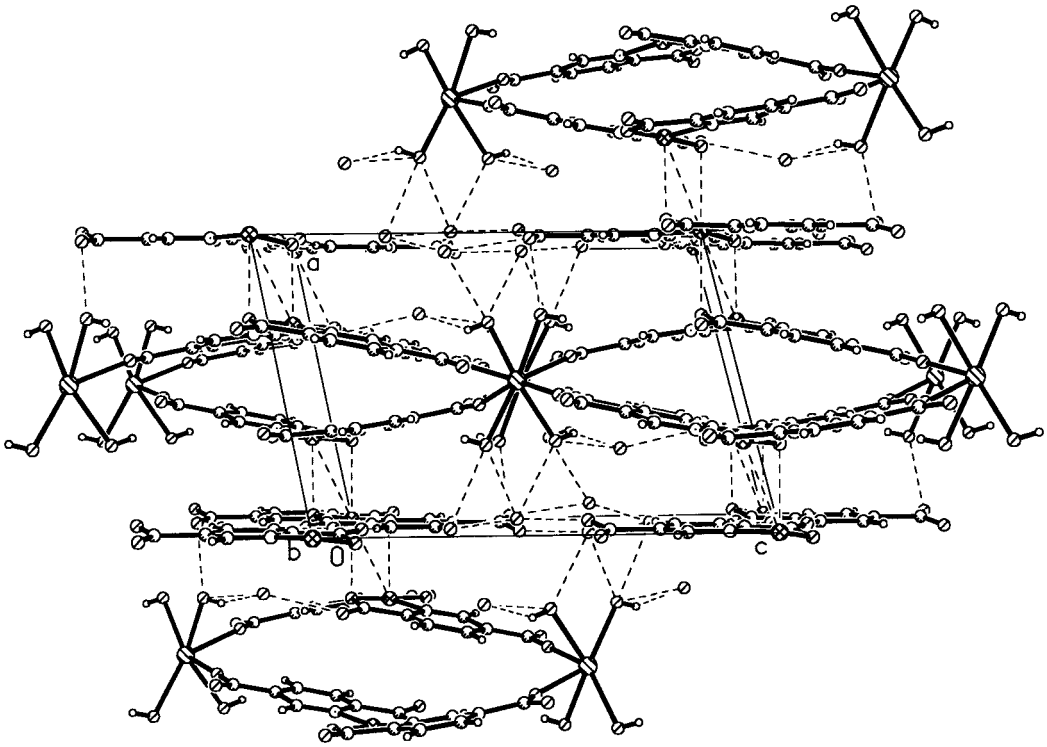

Figure 8. 3D packing structure of compound **6** along the *b* axis.

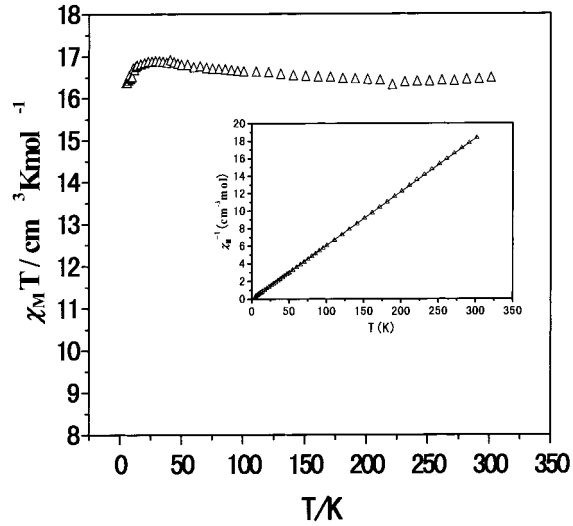

Figure 9. Experimental $\chi_M T$ versus T curves for complex **2**.

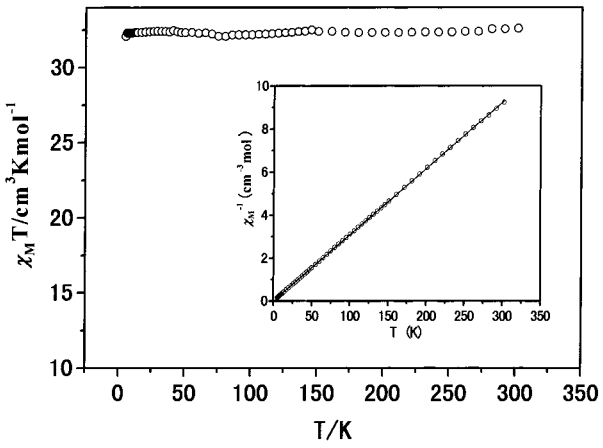

Figure 10. Experimental $\chi_M T$ versus T curves for complex **4**.

structure of the cation, which is made up of the $[Gd_2Cu_2(pydc)_4(H_2O)_8]$ building blocks, is very different from those in **1**−**5**. For clarity, it can be further viewed as $[Cu(pydc)_2]$ building blocks connected by gadolinium(III) linkers, where each copper(II) atom is chelated by two pydc ligands through a nitrogen atom and one oxygen atom of its adjacent carboxylate group in a distorted square planar geometry with O(23)−Cu(2)−O(33) and N(2)−Cu(2)−N(3) angles being 177.9(5) and 162.9(6)°, respectively, and the dihedral angle between two mean plane of Cu(2)N(2)O(23) and Cu(2)N(3)(33) being 17.4°. The average Cu−N (1.968 Å) and Cu−O (1.922 Å) values are similar to those in **1**−**5**. Each gadolinium(III) center was coordinated by eight oxygen atoms, four from four different pydc ligands and four from coordination water molecules with Gd−O bond lengths ranging from 2.301(10) to 2.458(12) Å. pydc ligands adopt a tridentate chelating-bridging coordination mode linking one copper(II) and two gadolinium(III) centers (Figure 3d). Hence, each $[Cu(pydc)_2]$ unit in the cation attaches to two gadolinium(II) linkers and each gadolinium(III) linker connects four $[Cu(pydc)_2]$ units, inducing a 2-D layer structure (Figure 7). The discrete $[Cu(pydc)_2]$ anion units are inserted between two cation layers, generating a sandwichlike structure which are further linked by hydrogen bond interactions of the water molecule and uncoordinated oxygen atoms of the carboxylate group to yield a 3-D structure (Figure 8). Although the Gd−Gd, Cu(2)−Cu(2), and Gd−Cu(2) distances in the cation are 5.285, 6.229, and 7.385 Å, revealing the lack of metal−metal interactions, the distance of Cu(1)−Cu(2) between anion and cation layers is 3.410 Å, indicating the possible existence of weak interaction between layers.

Magnetism of Complexes 2, 4, and 5. The temperature-dependent magneticsusceptibility data for **2**, **4**, and **5** are shown in Figures 9−11, respectively. For **2**, $\chi_M T$ is 15.92 cm^3 K mol^{-1} at 301.55 K and essentially keeps constant down to 50 K, slightly increases from 50 K, and reaches its maximum value of 16.87 cm^3 K mol^{-1} around 40.98 K, and then the value slightly decreases as T is lowered further. The experimental

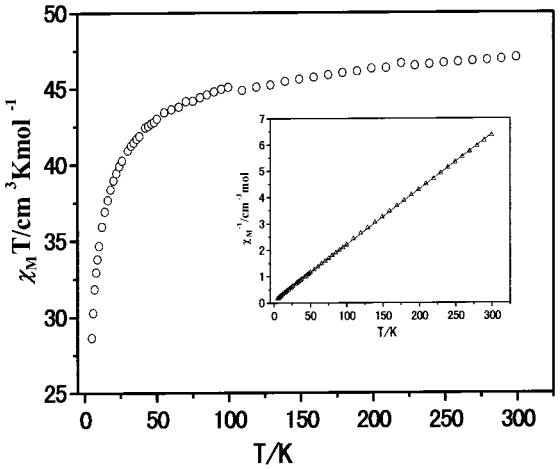

Figure 11. Experimental $\chi_M T$ versus T curves for complex **5**.

effective magnetic moments (μ_{eff}) were 11.47 μ_B at room temperature, which is very close to the theoretical value 11.62 μ_B (two Gd(III) and three Cu(II)), indicating nonmagnetic exchange interaction between adjacent Gd ions and Cu ions (only because the distances of Gd−Gd, Gd−Cu, and Cu−Cu between the adjacent units are 6.290, 5.801, and 5.119 Å, respectively). In the $1/\chi_M$ versus T plot (insert of Figure 8), the observed susceptibility data are well-fitted to the Curie−Weiss law ($\chi_M = C/(T - \Theta)$), with Weiss constant $\Theta = 0.7857$ K and $C = 16.3642$ K cm^3 mol^{-1}. For **4**, the values of $\chi_M T$ are essentially constant from 300 to 5 K (average value 32.33(20) cm^3 K mol^{-1}). The experimental effective magnetic moment (μ_{eff}) was 16.15 μ_B at room temperature, which is very close to the theoretical value 16.06 μ_B (four Gd(III) and two Cu(II)), indicating nonmagnetic exchange interaction between Gd(III) ions and Cu(II) ions of the adjacent units. The observed susceptibility data are well-fitted to the Curie−Weiss law ($\chi_M = C/(T - \Theta)$), with Weiss constant $\Theta = -0.28658$ K and $C = 32.46348$ K cm^3 mol^{-1}. For **5**, the $\chi_M T$ value is 47.05 cm^3 K mol^{-1} at 299.09 K and then declines slowly from 299.09 to 50 K. As temperature is further lowered, $\chi_M T$ values sharply reduce to 28.64 cm^3 K mol^{-1} at 5 K. The susceptibility magnetic data also obey the Curie−Weiss law with $C = 47.48$ cm^3 K mol^{-1} and $\Theta = -4.801$ K, showing antiferromagnetic interactions.

In conclusion, we have successfully constructed six Cu(II)−Ln(III) polymers by pyridine-2,5-dicarboxylic acid in hydrothermal reactions; the different forms of Cu(II) reagents along with the crystal growth conditions control the structures of the products. The work may supply a useful method of adjusting the metal/metal ratio and controlling the coordination mode of organic ligands for designing model complexes of magnetic materials.

Acknowledgment. This work was supported by grants from the National Natural Science Foundation of China, the Key Project from the Chinese Academy of Science, and the Superintendent Foundation of this Institute.

Supporting Information Available: X-ray crystallographic data, in CIF format, for the structure determinations of **1**−**6**. These materials are available free of charge via the Internet at http://pubs.acs.org.

IC0100929